CHAPTER VII *ELASTICITY THEORY OF DISLOCATIONS*

7.1 Introduction

As we saw in the previous chapter, in most cases, plastic deformation of a metal occurs through the propagation of dislocations. These dislocations can be introduced during crystal formation, that is, they exist before deformation, or they can be created during plastic deformation. In any case, each dislocation generates an elastic displacement field corresponding to elastic strains. These strains persist in the crystal even after the external stresses are removed. These are generally defined as internal stresses." Thus, dislocations lead to the storage of internal elastic energy in the crystal.

The variation of this energy with the position of dislocations is associated with self-interaction or interaction with other defects. The knowledge of these interactions allows us to evaluate the force:

- of the interactions between dislocations;
- of the one created by external stress on a dislocation.

Accordingly, we first calculate the stress and strain fields induced by a dislocation, along with the corresponding elastic energy (for an isotropic cubic crystal).

The displacements ($\vec{u}$) and the elastic stresses ($\overline{\overline{\sigma}}$) have to satisfy the three following conditions:

i) Satisfy Navier's equilibrium equation (3.77)

$$(1-2\nu)\Delta\vec{u} + \overrightarrow{grad}(div(\vec{u})) = 0$$

ii) Conserve $\vec{b}$ along the dislocation line.

$$\vec{b} = \oint \frac{\partial u}{\partial x} dx$$

iii) The external surfaces must be free of any force or moment.

$$\sigma_{ij}(M) dS_j = 0$$

7.2 Stress field around a dislocation

We consider a cylinder with axis Oz and create a dislocation line parallel to Oz by cutting through the plane xOz. We have a translational symmetry along z, and - as a consequence - all stresses, strains, and the $\vec{u}$ vector must be independent of z, meaning that all derivatives with respect to z must be equal to zero. Navier equilibrium equation (3.77) for the displacement field $\vec{u}$,

$$(1-2\nu)\Delta\vec{u} + \overrightarrow{grad}(div(\vec{u})) = 0$$

It can be written in Cartesian coordinates:

$$\begin{aligned}
(1-2\nu)\left(\frac{\partial^2 u_x}{\partial x^2}+\frac{\partial^2 u_x}{\partial y^2}\right)+\left(\frac{\partial^2 u_x}{\partial x^2}+\frac{\partial^2 u_y}{\partial x\partial y}\right)=0\\
(1-2\nu)\left(\frac{\partial^2 u_y}{\partial x^2}+\frac{\partial^2 u_y}{\partial y^2}\right)+\left(\frac{\partial^2 u_x}{\partial y\partial x}+\frac{\partial^2 u_y}{\partial y^2}\right)=0\\
\frac{\partial^2 u_z}{\partial x^2}+\frac{\partial^2 x_z}{\partial y^2}=0
\end{aligned} \qquad (7.1)$$

7.2.1 Screw dislocation

a) Infinite body (in the z-direction)

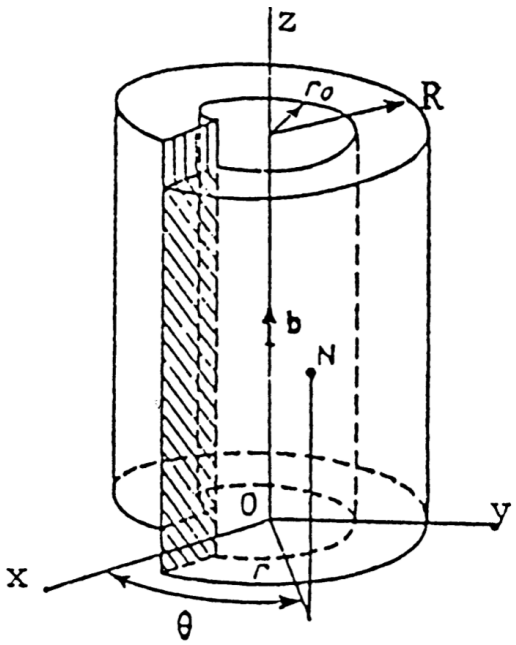

Figure 7-1: *Screw dislocation in a continuous body*

As a first approximation, we see that the displacement field $\vec{u}$ can be written intuitively in cylindrical coordinates (Figure 7-1) in the following way:

$$\begin{aligned}
u_r = r_\theta = 0\\
u_z = b\theta/2\pi
\end{aligned} \qquad (7.2)$$

In Cartesian coordinates:

$$u_x = u_y = 0$$
$$u_z = \frac{b}{2\pi}\arctan\frac{y}{x} \tag{7.3}$$

We can easily show that displacement satisfies conditions i) and ii).

The only non-zero components of the deformation tensor in Cartesian coordinates are then:

$$u_{xz} = \frac{1}{2}\left(\frac{\partial u_x}{\partial z} + \frac{\partial u_z}{\partial x}\right) = -\frac{b}{4\pi}\frac{y}{x^2+y^2}$$
$$u_{yz} = \frac{1}{2}\left(\frac{\partial u_y}{\partial z} + \frac{\partial u_z}{\partial y}\right) = \frac{b}{4\pi}\frac{x}{x^2+y^2}$$

Or, in cylindrical coordinates:

$$u_{\theta z} = \frac{1}{2}\left(\frac{\partial u_\theta}{\partial z} + \frac{\partial u_z}{r\,\partial\theta}\right) = \frac{b}{4\pi r} = u_{z\theta} \tag{7.4}$$

with all other components equal to zero:

$$u_{rr} = \frac{\partial u_r}{\partial r} \qquad u_{\theta\theta} = \frac{1}{r}\frac{\partial u_\theta}{\partial\theta} + \frac{u_r}{r} \qquad u_{zz} = \frac{\partial u_z}{\partial z}$$
$$u_{r\theta} = \frac{1}{2}\left(\frac{1}{r}\frac{\partial u_r}{\partial\theta} + \frac{\partial u_\theta}{\partial r} - \frac{u_\theta}{r}\right) \qquad u_{rz} = \frac{1}{2}\left(\frac{\partial u_r}{\partial z} + \frac{\partial u_z}{\partial r}\right)$$

The only non-zero components of the tensor $\overline{\overline{\sigma}}$ expressed in Cartesian coordinates (see equation (3.61)), are because the diagonal components of u_{ij} are zero.

$$\sigma_{xz} = 2\mu u_{xz} = -\frac{\mu b}{2\pi}\frac{y}{x^2+y^2}$$
$$\sigma_{yz} = 2\mu u_{yz} = \frac{\mu b}{2\pi}\frac{x}{x^2+y^2} \tag{7.5}$$

In cylindrical coordinates:

$$\sigma_{\theta z} = 2\mu u_{\theta z} = \frac{\mu b}{2\pi r} = \sigma_{z\theta} \tag{7.6}$$

b) Finite body (in the z-direction)

For a finite tube in the *z*-direction, the shear component $\sigma_{z\theta}(=\sigma_{\theta z})$ produces a torque between the two ends of the cylinder:

$$M_z = \int_0^{2\pi}\int_{r_0}^{R} r(\sigma_{z\theta} r\,dr\,d\theta) = \mu b\int_{r_0}^{R} r\,dr = \frac{\mu b}{2}(R^2 - r_0^2) \tag{7.7}$$

This means that condition iii) is not satisfied (forces and moments must be zero). Therefore, the previous solution for an infinite body is invalid. The strain tensor must be modified so that the stress vanishes on the external surfaces. Another deformation must be added for the corresponding surface stress:

$$\sigma'_{z\theta} = -\frac{\mu b}{2\pi r} = \sigma'_{\theta z} \tag{7.8}$$

and to a torque:

$$M'_z = -\frac{\mu b}{2}(R^2 - r_0^2) \tag{7.9}$$

This torque corresponds to the elastic stresses created by torsion in the sample (Figure 7-2). A new field $\vec{u}$ is produced, which must vary linearly with z and can be written:

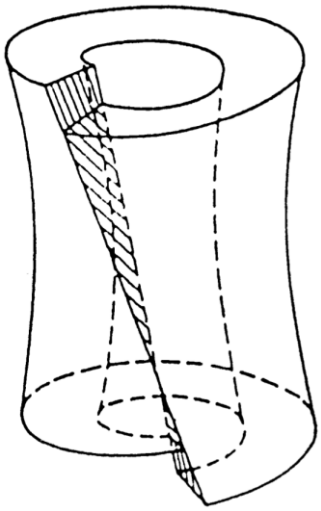

$u'_\theta(r,z) = -r\phi(z) = -Arz$ and $u'_r = u'_z = 0$

From which we deduce:
$u'_{z\theta} = -Ar/2 = u'_{\theta z}$

and by equation (7.6)
$\sigma'_{z\theta} = -\mu Ar = \theta'_{\theta z}$

which corresponds to the torque
$M'_z = -\int_0^{2\pi}\int_{r_0}^{R} r(\sigma'_{z\theta}\, r\, dr\, d\theta)$

Figure 7-2: *Screw dislocation in a finite body*

Now, let's assume:

$$M'_z = -2\pi\mu A\int_{r_0}^{R} r^3\, dr = -\frac{\pi\mu A}{2}(R^4 - r_0^4)$$

The constant A is obtained by writing that the sum of the torques due to $\bar{\bar{\sigma}}$ and $\bar{\bar{\sigma}}'$ is zero. That is:

$$M_z + M'_z = 0 \rightarrow A = \frac{b}{\pi}\frac{R^2 - r_0^2}{R^4 - r_0^4} \tag{7.10}$$

and considering that $R >> r_0$

$$A \approx b/\pi R^2$$

and finally:

$$u_{\theta z} = u_{z\theta} = \frac{b}{4\pi r}\left(1 - \frac{2r^2}{R^2}\right) \quad \text{and} \quad \sigma_{\theta z} = \sigma_{z\theta} = \frac{\mu b}{2\pi r}\left(1 - \frac{2r^2}{R^2}\right) \tag{7.11}$$

7.2.2 Edge dislocation

a) General case

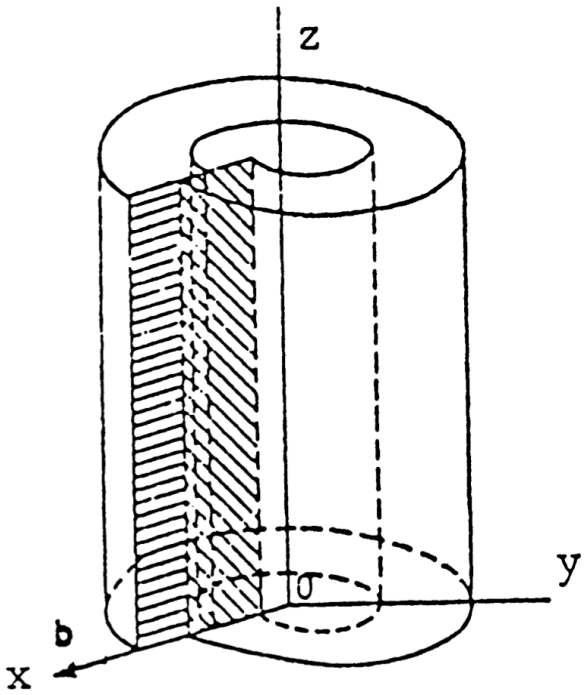

Figure 7-3: *Dislocation in a continuous body*

The displacement field is not as simple as before. However, in a general way, we show (cf. Hirth & Lothe, pages 71-74) that the displacement field $\vec{u}$ satisfying the three conditions i), ii), and iii) can be written in Cartesian coordinates:

$$u_x = \frac{b}{2\pi}\left\{\theta + \frac{1}{4(1-\nu)}\left[1 + \frac{(3-4\nu)r^2}{R^2+r_0^2} - \frac{R^2 r_0^2}{r^2(R^2+r_0^2)}\right]\sin 2\theta\right\}$$

$$u_y = -\frac{b}{8\pi(1-\nu)}\left\{2(1-2\nu)lnr + \frac{2r^2}{R^2+r_0^2} + \left[1 + \frac{(3-4\nu)r^2}{R^2+r_0^2} - \frac{R^2 r_0^2}{r^2(R^2+r_0^2)}\right]\cos 2\theta\right\}$$

and obviously $u_z = 0$.

b) Simplified case

The previous relations can be simplified for boundary conditions of infinite continuous ($r = r_0$ and $r = R$), such that:

$$u_x = \frac{b}{2\pi}\left(\theta + \frac{\sin 2\theta}{4(1-\nu)}\right)$$

$$u_y = -\frac{b}{2\pi}\left(\frac{1-2\nu}{2(1-\nu)}\ln r^2 + \frac{\cos 2\theta}{4(1-\nu)}\right) \qquad (7.12)$$

Let: $D = \frac{\mu b}{2\pi(1-\nu)}$; the stress tensor $\bar{\bar{\sigma}}$ is in Cartesian coordinates:

$$\sigma_{xx} = -D\frac{\sin\theta(2+cos2\theta)}{r} \qquad \sigma_{yy} = D\frac{\sin\theta cos2\theta}{r} \qquad \sigma_{zz} = -2D\nu\frac{\sin\theta}{r} \tag{7.13}$$

$$\sigma_{xy} = D\frac{\cos\theta cos2\theta}{r} \qquad \sigma_{xz} = \sigma_{yz} = 0$$

In cylindrical coordinates:

$$\sigma_{rr} = \sigma_{\theta\theta} = -D\frac{\sin\theta}{r} \qquad \sigma_{zz} = -2D\nu\frac{\sin\theta}{r} \tag{7.14}$$

$$\sigma_{r\theta} = D\frac{\cos\theta}{r} \qquad \sigma_{rz} = \sigma_{\theta z} = 0$$

Inserting these expressions in Hooke s law (Chapter 3 Eqn. 3.69):

$$u_{ij} = \frac{1}{2\mu}\left(\sigma_{ij} - \frac{\nu}{1+\nu}\sigma_{kk}\delta_{ij}\right)$$

We can get the components of the strain tensor in cylindrical coordinates:

$$u_{rr} = u_{\theta\theta} = \frac{D(1-2\nu)}{2\mu}\frac{\sin\theta}{r}, \qquad u_{r\theta} = -\frac{D}{2\mu}\frac{\cos\theta}{r}, \qquad u_{zz} = u_{\theta z} = u_{rz} = 0 \tag{7.15}$$

Remarks:

- In any case, the stresses decrease as 1/r, and they diverge when $r \to 0$
- The stress tensor corresponding to screw and edge dislocations is orthogonal in an infinite body

7.3 Elastic energy

A stress and strain field around a dislocation implies that a specific elastic energy is embedded within the crystal. In the framework of Hooke s law (linearity between stresses and strains - equation (3.69)), the elastic energy stored per unit volume can be written as:

$$w = \frac{1}{2}\sigma_{ij}u_{ij} \tag{7.16}$$

The energy of a dislocation line can then be calculated knowing $\bar{\bar{\sigma}}$ and $\bar{\bar{u}}$ using $W = \frac{1}{2}\int \sigma_{ij}u_{ij}\,dV$

7.3.1 Screw dislocation

The energy density for a screw dislocation of finite length is given by:

$$w = \frac{1}{2}(\sigma_{\theta z}u_{\theta z} + \sigma_{z\theta}u_{z\theta}) = \frac{\mu b^2}{8\pi^2 r^2}\left(1 - \frac{2r^2}{R^2}\right)^2 \tag{7.17}$$

We can then calculate the stored energy of a dislocation line *per unit length* by integrating over the volume of an elastic cylinder of a unit length between the radius r_0 and R:

$$W = \int_0^1 dz \int_0^{2\pi} d\theta \int_{r_0}^{R} wr\, dr = \int_{r_0}^{R} \frac{\mu b^2}{4\pi r}\left(1 - \frac{2r^2}{R^2}\right)^2 dr$$

This integral yields:

$$W = \frac{\mu b^2}{4\pi}\left[\ln r - 2\frac{r^2}{R^2} + \frac{r^4}{R^4}\right]_{r_0}^{R}$$

and since $R >> r_0$

$$W \approx \frac{\mu b^2}{4\pi}\left(\ln\frac{R}{r_0} - 1\right) \tag{7.18}$$

and in the case of a screw dislocation in an infinite cylinder, we have (you can derive it as an exercise):

$$W = \frac{\mu b^2}{4\pi}\ln\frac{R}{r_0} \tag{7.19}$$

Remarks:

- W has dimensions of energy per unit length.
- The difference between the case of an infinite and a finite body is the relaxation occurring on the surfaces, which decreases this energy.
- W goes to infinity when r_0 goes to zero. Since the stress tensor of the dislocation core is unknown, the total energy is usually written as $W_t = W + W_0$, where W_0 corresponds to the energy at the dislocation core $(r < r_0)$.

The value given to W_0 is discussed in § 7.3.4.

7.3.2 Edge dislocation

In this case, the energy density is (simplified case):

$$w = \frac{1}{2}(\sigma_{rr}u_{rr} + \sigma_{\theta\theta}u_{\theta\theta} + \sigma_{r\theta}u_{r\theta} + \sigma_{\theta r}u_{\theta r})$$

That is, using the previous expressions of $\overline{\overline{\sigma}}$ and $\overline{\overline{u}}$ (7.2.2 b):

$$w = \frac{\mu b^2}{8\pi^2(1-\nu)^2}\left(\frac{1 - 2\nu\sin^2\theta}{r^2}\right) \tag{7.20}$$

and integrating as before:

$$W = \int_0^1 dz \int_{r_0}^{R}\int_0^{2\pi} wr\, dr\, d\theta = \left(\frac{\mu b^2}{4\pi(1-\nu)^2} - \frac{\nu\mu b^2}{4\pi(1-\nu)^2}\right)\ln\frac{R}{r_0}$$

We finally get:

$$W = \frac{\mu b^2}{4\pi(1-\nu)}\ln\frac{R}{r_0} \tag{7.21}$$

As for the screw dislocation, the total energy is equal to $W_t = W + W_0$, where W_0 corresponds to the energy of the dislocation core.

Remarks:

• In general, ν ~1/3 → the energy of an edge dislocation is slightly higher than that of a screw dislocation.

• The elastic energy increases as *R* goes to infinity. Although *R* is finite (the boundary of the crystal), the energy associated with it is relatively high. In common metals, this energy cost ranges between 5 and 10 eV for an atomic plane cutting through a dislocation line. As such, dislocations cannot spontaneously appear by thermal agitation (thus, dislocations do not correspond to states of thermodynamic equilibrium of the crystal).

7.3.3 Mixed dislocation

In the case of a mixed dislocation for which $\vec{b}$ forms and angle ψ with ξ, it is sufficient to take the screw and edge components of $\vec{b}$ and add their contributions for both types of dislocations (the respective stress tensors being orthogonal) so that we have:

$$W = \frac{\mu}{4\pi}\left(b_v^2 + \frac{b_c^2}{1-\nu}\right)\ln\frac{R}{r_0} = \frac{\mu b^2}{4\pi}\ln\frac{R}{r_0}\left(\cos^2\psi + \frac{\sin^2\psi}{1-\nu}\right)$$

In a more compact form:

$$W = \frac{\mu b^2}{4\pi(1-\nu)}(1-\nu\cos^2\psi)\ln\frac{R}{r_0} \qquad (7.22)$$

Remark:

We note here that in classic elasticity theory, the elastic energy W of dislocation is, no matter its type, proportional to b^2. This means that, for any crystal structure, only a few Burgers vectors, corresponding to the shortest lattice translations, generate stable dislocations. The other dislocations tend to dissociate spontaneously into more stable elements.

7.3.4 The problem of the dislocation core

Until now, we have considered that when r → 0, the dislocation is at the center of an empty cylinder of internal radius r_0.

What happens in a perfect crystal? The linear elastic relations can be considered valid for values of strain up to ε ~10% (i.e., until stress equivalent to the theoretical maximum yield stress, σ=μ/10, that was calculated in § 6.2.1), which corresponds for a screw dislocation to a core radius of:

$$2u_{z\theta} = \frac{b}{2\pi}\frac{1}{r_c} = 0.1 \Rightarrow r_c \approx 2b$$

a) Case of a filled core

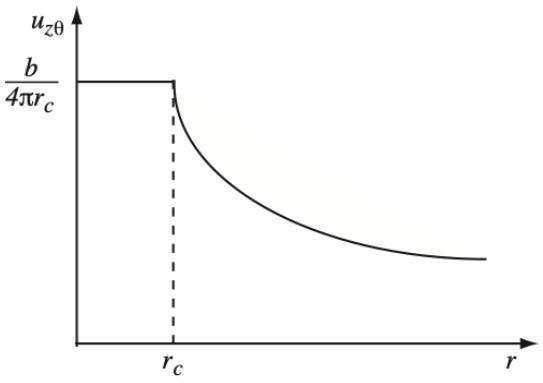

Figure 7-4: *Deformation of the core*

In this case, a lower bound on the core energy can be estimated by assuming that the deformation in the central zone is uniform and equal to the one for $r = r_c$ (Figure 7-4), for example, for a screw dislocation of infinite length, such that:

$$W_0 = \frac{1}{2}(2\sigma_{z\theta}u_{z\theta})\pi r^2 \qquad \text{per unit length.}$$

Using (7.4) and (7.6)

$$W_0 = \frac{\mu b^2}{8\pi^2 r_c^2}\pi r_c^2 = \frac{\mu b^2}{8\pi} \tag{7.23}$$

The upper limit is the one that corresponds to the latent heat of fusion of a unit-length cylinder of radius r_c - $W_0 \sim \mu b^2 / 5$ (L. Bragg, *Symposium on internal stresses*, London, 1948), with an average value around the mean:

$$W_0 = \approx \frac{\mu b^2}{5\pi}$$

The total energy of a screw dislocation in a finite body is then equal to:

$$W_t = W + W_0 = \frac{\mu b^2}{4\pi}\left(\left(ln\frac{R}{r_c}\right) + \frac{4\pi}{5\pi}\right) = \frac{\mu b^2}{4\pi}\left(ln\frac{R}{b} + ln\frac{b}{r_c} + \frac{4\pi}{5\pi}\right) \simeq \frac{\mu b^2}{4\pi} ln\frac{R}{b} \tag{7.24}$$

This corresponds to considering a filled core dislocation in a crystal equivalent to a dislocation with an empty core of radius b in a continuous elastic body. The formula (7.24) constitutes a good approximation of the energy of a screw dislocation. For a general dislocation, work can be defined as,

$$W = \frac{\mu b^2}{4\pi K}\ln\frac{R}{b} \tag{7.25}$$

$$\text{with } K = \frac{1-\nu}{1-\nu cos^2\psi}$$

b) Hollow core dislocation

We consider now the case of an extended core:

$$W = \frac{\mu b^2}{4\pi}\ln\frac{R}{r} + 2\pi r\gamma$$

where γ is the surface energy of the crystal, and we assume implicitly that $r \geq r_c$. This energy has a minimum.

$$\left(\frac{\partial W}{\partial r}\right)_{r=r_0} = 0$$

which corresponds to the following:

$$r_0 = \frac{\mu b^2}{8\pi^2\gamma} \approx \frac{b^2}{8a} \tag{7.26}$$

where we assumed that the surface energy is $\gamma \approx a\frac{\mu}{10} =$ theoretical elastic yield stress (where a is the lattice constant), corresponding to the cleavage energy. It is clear that to have a hollow core dislocation, $r_0 \geq a$, which according to (7.26) becomes $b \geq 2\sqrt{2}a$. Thus, dislocations with hollow cores have large Burgers vectors.

7.4 Interaction energy between dislocations

We should distinguish between the self-energy of a dislocation and the interaction energy between two dislocations. For example, consider a solid containing two dislocations, A and B, responsible for the stress fields σ_{ij}^A and σ_{ij}^B and the strain fields u_{ij}^A and u_{ij}^B. The superposition principle dictates:

$$\begin{aligned} \sigma_{ij} &= \sigma_{ij}^A + \sigma_{ij}^B \\ u_{ij} &= u_{ij}^A + u_{ij}^B \end{aligned} \tag{7.27}$$

As a consequence, the total energy becomes:

$$E = \frac{1}{2}\int_V \sigma_{ij}^A u_{ij}^A \, dV + \frac{1}{2}\int_V \sigma_{ij}^B u_{ij}^B \, dV + \frac{1}{2}\int_V \sigma_{ij}^A u_{ij}^B \, dV + \frac{1}{2}\int_V \sigma_{ij}^B u_{ij}^A \, dV \tag{7.28}$$

The first two terms represent the self-energy of each dislocation. The last two terms are equal because of Hooke s law (you can prove this statement as an exercise), and their sum represents the interaction energy.

$$E_I = \int_V \sigma_{ij}^A u_{ij}^B \, dV = \int_V \sigma_{ij}^B u_{ij}^A \, dV \tag{7.29}$$

For calculating this integral, consider a dislocation loop A with contour C and a general surface S bounded by this loop (Figure 7-5). We define a normal vector $\vec{n}$ on this surface.

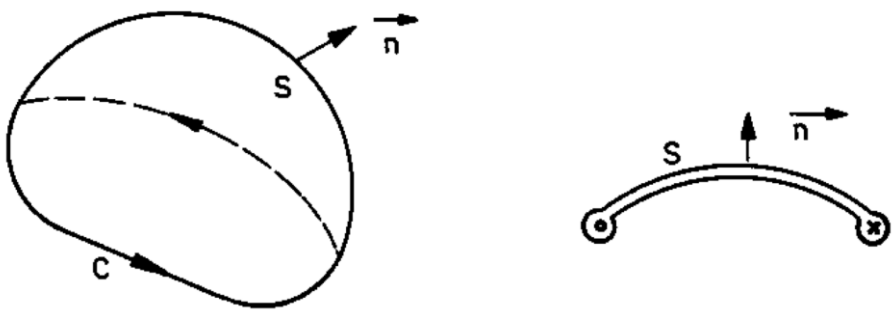

Figure 7-5: *Surface S encircling the integration contour C*

Dislocation A was obtained by cutting along a general surface delimited by contour C and moving one side with respect to the other by a distance $\overrightarrow{b^A}$. Our integral can then be evaluated on a volume bounding the sliding surface, keeping in mind that $\sigma_{ij} = \sigma_{ji}$:

$$E_I = \int_V \sigma_{ij}^B u_{ij}^A \, dV = \int_V \sigma_{ij}^B \beta_{ij}^{\ A} dV = \int \left(\frac{\partial}{\partial x_j}\left(\sigma_{ij}^B u_i^{\ A}\right) - \frac{\partial \sigma_{ij}^B}{\partial x_j} u_i^A \right) dV \qquad \text{where } \beta_{ij} = \frac{\partial u_i}{\partial x_j}$$

By the equilibrium equation (3.26), $\frac{\partial \sigma_{ij}}{\partial x_j} = 0$

Applying the divergence theorem

$$E_I = \int_S \sigma_{ij}^B u_{ij}^A \, dS_j$$

If we take the surface drawn in Figure 7-5, the side that has slipped (for example, the top surface) gives $\overrightarrow{u^A} = \overrightarrow{b^A}$ and the other $\overrightarrow{u^A} = 0$, so that:

$$E_I = b_i^A \int_S \sigma_{ij}^B \, dS_j = \overrightarrow{b^A} \cdot \int_S \overline{\overline{\sigma^B}}\, \overrightarrow{dS} \tag{7.30}$$

7.5 Force on a dislocation

7.5.1 Definition

Knowing the interaction energy E_I between two dislocations makes it possible to calculate the force applied by one dislocation on the other, which is given by:

$$\vec{F} = -\vec{\nabla} E_I$$

Let $\vec{L}$ be a loop with a Burgers vector $\vec{b}$, the variation in energy dE_I when an element $d\vec{L}$ is displaced over a distance $\overrightarrow{dl}$ by an external stress $\overline{\overline{\sigma}}$ is (Figure 7-6):

$$dE_I = \vec{b}(\overline{\overline{\sigma}} \cdot d\vec{S}) = (\vec{b} \cdot \overline{\overline{\sigma}}) d\vec{S} = (\vec{b} \cdot \overline{\overline{\sigma}})(\overrightarrow{dl} \wedge \overrightarrow{dL})$$

Using:

$$\vec{x} \cdot (\vec{y} \wedge \vec{z}) = (\vec{x} \wedge \vec{y}) \cdot \vec{z}$$

We get:

$$dE_I = -[(\vec{b} \cdot \overline{\overline{\sigma}}) \wedge \overrightarrow{dL}] \cdot \overrightarrow{dl}$$

As the variation dE_I does not depend on the displacement $\overrightarrow{dl}$ of the arc $\overrightarrow{dL}$ we have: $dE_I = -\vec{F} \cdot \overrightarrow{dl}$

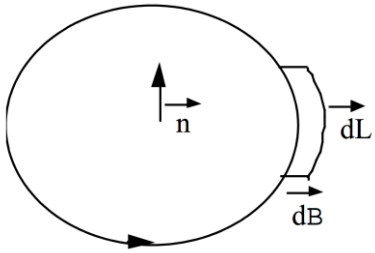

Figure 7-6: *Strain of a dislocation loop*

We obtain then:

$$d\vec{F} = (\vec{b} \cdot \bar{\bar{\sigma}}) \wedge \overrightarrow{dL}$$

As such, for a dislocation portion of length L, the force is:

$$\vec{F} = (\vec{b} \cdot \bar{\bar{\sigma}}) \wedge \vec{L} \tag{7.31}$$

That is, $\vec{F}$ the force required to move the dislocation under the external stress $\bar{\bar{\sigma}}$ in Eqn. 7.31 is called the Peach and Koehler equation. This relation indicates that the force is perpendicular to the line element, confirming the intuition that a displacement along the dislocation line does not affect the system's configuration.

7.5.2 Applications

a) Forces acting on a dislocation

Consider an edge dislocation determined by the right-handed Cartesian coordinate system ($\xi, \vec{b}, \vec{n}$) as defined previously in § 6.2.3. For example, we then have the following (Figure 7-7):

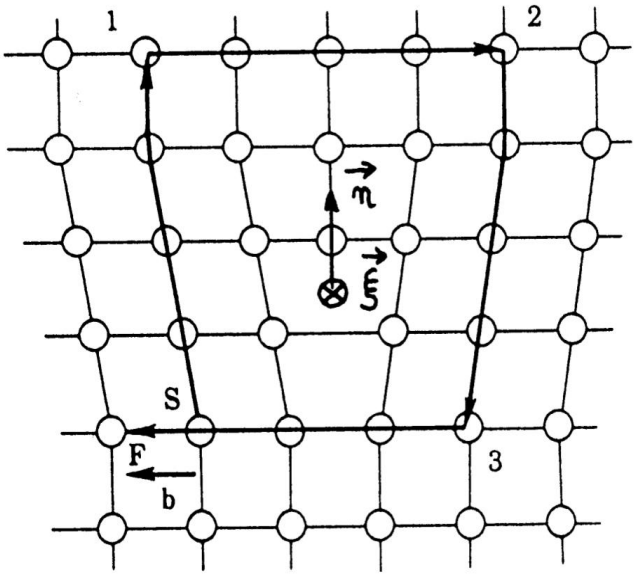

• A force in the perpendicular plane to the glide plane, defined by its normal $\vec{n}$ and equal to:

$F_{\perp} = ((\vec{b} \cdot \bar{\bar{\sigma}}) \wedge \vec{\xi}) \cdot \vec{n}$

This is a climb force at high temperatures.

• A force parallel to the dislocation line:

$F_{//} = ((\vec{b} \cdot \bar{\bar{\sigma}}) \wedge \vec{\xi}) \cdot \vec{\xi} = 0$

• A force in the glide plane:

$$F_p = ((\vec{b} \cdot \bar{\bar{\sigma}}) \wedge \vec{\xi}) \cdot \frac{\vec{b}}{|\vec{b}|} = (\vec{b} \cdot \bar{\bar{\sigma}}) \cdot \vec{n}$$

or else $F_p = \sigma_{ij} b_i n_j$

Figure 7-7: *Direct trihedron of the dislocation*

The last expression for F_p means only the shear stresses can move the dislocation in its glide plane.

b) Interaction between two parallel screw dislocations

Consider two parallel screw dislocations with Burgers vectors $\vec{b_1} = (0,0,b_1)$ and $\vec{b_2} = (0,0,b_2)$ respectively (Figure 7-8).

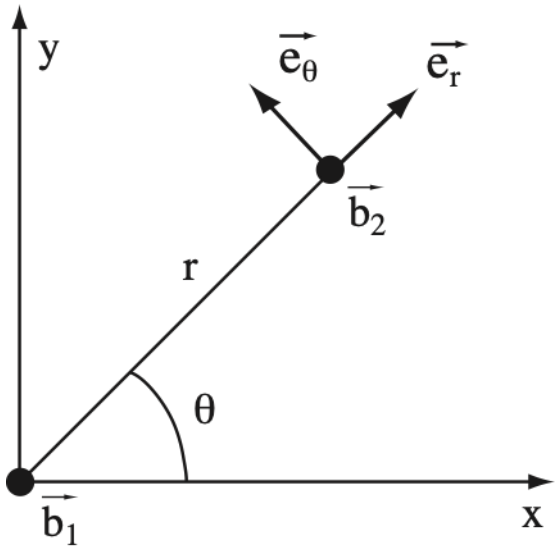

Figure 7-8 : *Interaction between two screw dislocations*

The stress field due to the dislocation with Burgers vector $\vec{b}_1$ is given by: $\sigma_{\theta z} = \frac{\mu b_1}{2\pi r}$, which corresponds respectively to a radial force between the two dislocations:

$$F_r = b_2 \sigma_{\theta z} = \frac{\mu b_1 b_2}{2\pi r}$$

and a tangential force: $F_\theta = 0$.

Considering that $|\vec{b}_1| = |\vec{b}_2|$ we can simplify this in:

$$F_r = \pm \frac{\mu b^2}{2\pi r} \qquad (7.32)$$

This is equivalent to saying that dislocations attract or repel each other depending on whether they have opposite or equal signs.

c) Interaction between two parallel edge dislocations

Consider two edge dislocations with Burgers vectors $\vec{b}_1 = (b_1, 0, 0)$ and $\vec{b}_2 = (b_2, 0, 0)$ respectively (Figure 7-9). The two dislocation lines are aligned with the z-axis so that the only components of the interaction forces that count are those in the *x* and *y* directions:

$$F_x = b_2 \sigma_{xy} \text{ and } F_y = -\sigma_{xx} b_2$$

The force component in the glide plane is then (exercise):

$$F_x = b_2 \sigma_{xy} = \frac{\mu b_2 b_1}{2\pi K} \frac{\cos\theta cos2\theta}{r} \qquad (7.33)$$

The climb component perpendicular to the glide plane is:

$$F_y = \frac{\mu b_1 b_2}{2\pi K} \frac{\sin\theta(2+\cos 2\theta)}{r}$$

Note here that this climb force acts effectively only at high temperatures ($T > T_f/2$ where T_f is the melting point or fusion temperature in the notation) as the displacement of the dislocation line out of its glide plane requires absorption or emission of point defects, which are formed much faster at high temperatures. Considering that the two dislocations are confined in their glide plane (no climb assumed), the equilibrium positions of these two dislocations correspond to $F_x = 0$, that is:

$$\cos\theta = 0 \Rightarrow \theta = \frac{\pi}{2}, \cos 2\theta = 0 \Rightarrow \theta = \frac{\pi}{4} \text{ and } r \to \infty \Rightarrow \theta \sim 0$$

which are not all stable equilibrium positions. It is clear that the stability of these equilibrium positions depends on the sign of $\vec{b}_1 \cdot \vec{b}_2$, that is:

• If the two dislocations have the same sign, $\vec{b_1} \cdot \vec{b_2} > 0$ and the stable equilibrium positions correspond to:

- $\theta = 0$ or π, the two dislocations are at infinity, one from the other; $\theta = \pi/2$, the two dislocations are in the same plane, that is, one underneath the other.

• If the two dislocations have opposite signs (dipole), $\vec{b_1} \cdot \vec{b_2} < 0$ and the equilibrium positions correspond to $\pm\theta = \pi / 4$.

Any other position is *unstable*.

7.5.3 interaction with surfaces: image forces

In the previous sections, we simplified the calculations by assuming that dislocations were distributed throughout an infinite body, thereby neglecting surface effects. However, when a dislocation is close to the surface, what are the stress fields of a dislocation in a crystal of finite dimensions? What is the interaction between dislocations and surfaces?

Consider a semi-infinite body limited by a free surface S and a screw dislocation parallel to this surface and situated at a distance *d*. We saw that the self-energy of a screw dislocation is given by (7.24):

$$W = \frac{\mu b^2}{4\pi K} \ln \frac{R}{b} \approx \frac{\mu b^2}{4\pi K} \ln \frac{d}{b}$$

Therefore, the self-energy of this dislocation decreases with distance *d* from the surface S to the dislocation, which is equivalent to saying that the surface attracts the dislocation. The attractive force can be calculated by considering the boundary condition that the surface S is stress-free.
For this case, consider two parallel screw dislocations, A and B, at a distance (d) and with opposite $\vec{b}$ vectors (dipole) in an infinite body with a shear modulus μ. We can calculate the stress and strain tensors at any point M of this body, and we note that there are no stresses on the median plane between the two dislocations.

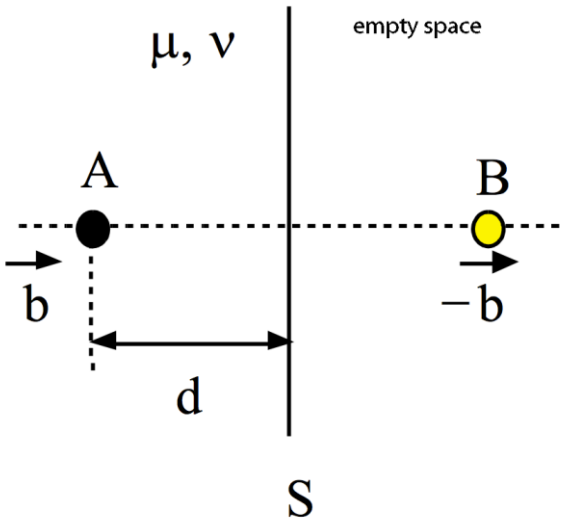

Figure 7-10 : *The dislocation A is attracted by its image B and thus by the surface*

We can then cut along this plane without introducing new stresses, leaving us with the initial problem of a single screw dislocation and a surface. In this configuration, dislocation B is referred to as the image of dislocation A.

Dislocation A is attracted by its image B with a force per unit length equal to (7.32):

$$F = \frac{\mu b^2}{4\pi d}$$

This force represents approximately the interaction force between the screw dislocation A and the surface S. A similar approach can be adopted for edge dislocations.

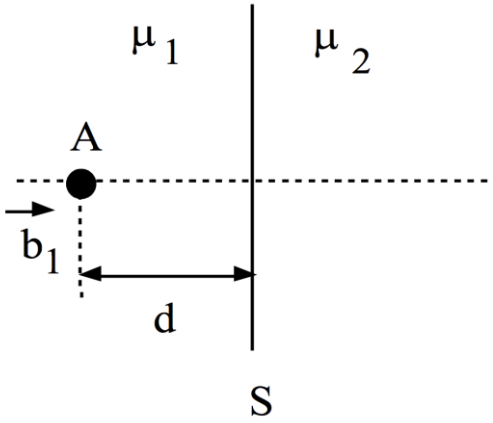

The elastic energy of a dislocation depends linearly on the elastic modulus of the body. Thus, if $\mu_1 > \mu_2$, the dislocation tends to move towards body 2; in the opposite case, it moves away from the interface.

Figure 7-10: *Interaction with a surface between two bodies with different elastic moduli*

7.5.4 The concept of line tension

A dislocation with a specific energy W per unit length tends to minimize its total energy by reducing its length. Similar to a soap bubble or a balloon that tends to reduce its surface area under surface tension, a dislocation loop tends to reduce its diameter due to a line tension τ in the direction of the line.

We attribute a dislocation line tension (τ) as the ratio between the energy variation *dW* and the variation in length that caused it, *dl*:

$$\tau = \frac{dW}{dl} = \lim_{\delta l \to 0} \frac{\delta W}{\delta l}$$

In other words, the line tension represents the tangential force, which should be applied at point M of the dislocation line to keep the same configuration after a cut in the line is made at point M.

7.5.5 Interpretation of the line tension

Consider an arc of dislocation AB, belonging to a dislocation loop with Burgers vector $\vec{b}$. The arc is at equilibrium in its glide plane and is submitted to external stress σ_0 (Figure 7-11).

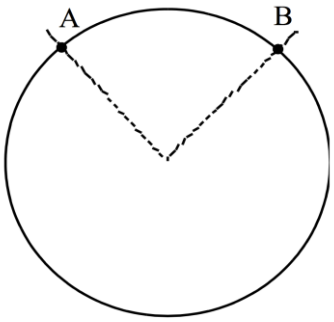

The force to which this arc is submitted because of the external stress, according to Peach and Koehler, is :

$$F_p = \sigma_0 b dl$$

Since the loop is considered at equilibrium, the segment AB is also at equilibrium, so that there is a restoring force (Figure 7-12):

$$F_r = -\sigma_0 b dl$$

Figure 7-11 : *Dislocation loop*

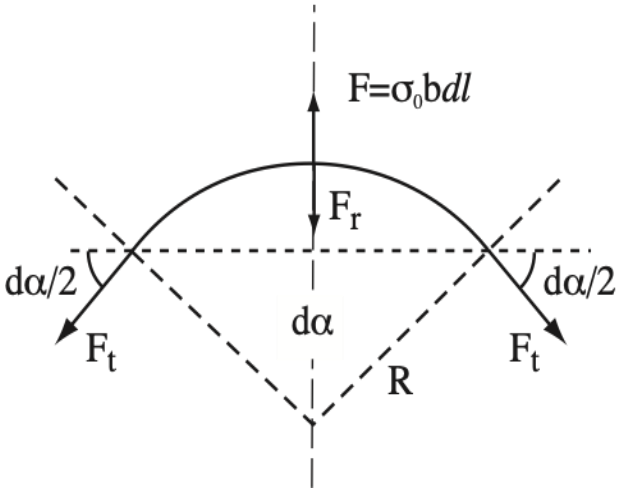

We can replace this restoring force with two tangential forces F_t acting at the two ends, A and B, of the arc of the dislocation, such that:

$$F_t = \frac{F_r}{2\sin(d\alpha/2)} \approx \frac{F_r}{d\alpha}$$

Considering the dislocation as an elastic line (approximation of the line tension), the work required to stretch the arc AB by a length *dl/2* from each side is:

$$dW = F_t dl \Rightarrow F_t = \frac{dW}{dl}$$ which means that $\tau = F_t$.

Figure 7-13: *Equilibrium of forces on an arc of dislocation*

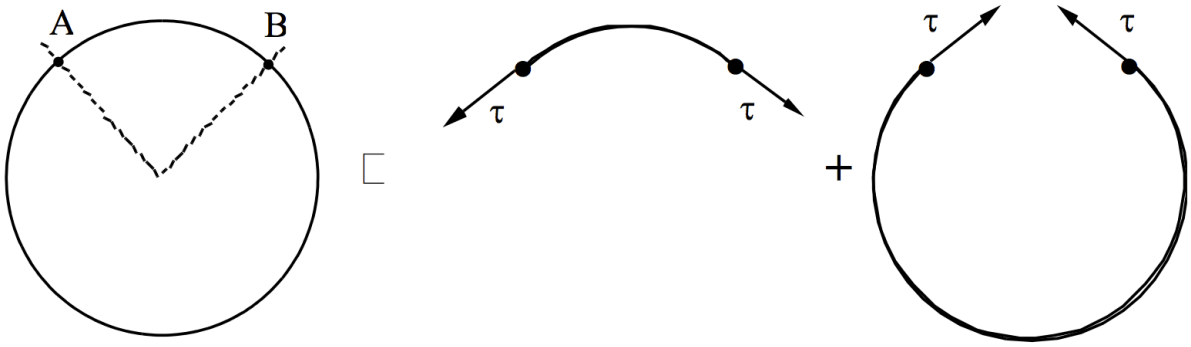

Figure 7-14: *Diagram showing the concept of line tension*

It is not hard to see that, if we neglect the variation in energy of the dislocation line according to the type of dislocation, the line tension τ is equal to the work (W) per unit length. We must remember that the energy calculated in (7.19) is a measure of energy per unit length:

$$W = \frac{\mu b^2}{4\pi K}\ln\frac{R}{b}$$

For an increase in length *dl*, $dW = \frac{\mu b^2}{4\pi K}\ln\frac{R}{b}dl$ and thus:

$$\tau = \frac{dW}{dl} = \frac{\mu b^2}{4\pi K}\ln\frac{R}{b} \qquad (7.34)$$

A value of $\tau \sim 0.5\,\mu b^2$ to $1\,\mu b^2$ is typically used as line tension in the framework of the classic isotropic theory.

7.5.6 Application: Frank-Read sources

Consider a segment of dislocation of initial length *l* (Figure 7-14), anchored to its two ends, A and B, and submitted in its glide plane to a shear stress σ_0. Under this stress, each element of length *dl* of this dislocation segment is subjected to a force /normal, which lies in the glide plane.

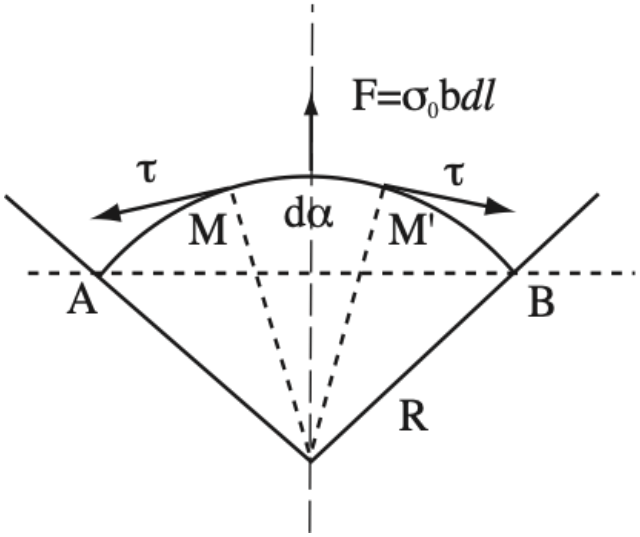

Figure 7-15 : *Equilibrium of forces and line tension on a dislocation arc*

According to the Peach and Koehler equation, the absolute value of this force is given by:

$$dF = \sigma_0 b dl$$

The problem comes down to determining the equilibrium configuration of an arc such as MM of length *dl* and submitted to a stress σ_0 (Figure 7-14). This arc is submitted to the force $\overrightarrow{dF}$ due to the stress σ_0 from one side and to the line tension from the other side, which is applied in M and M by the rest of the arc.

Let R be the curvature radius of the element MM and dα the angle it intercepts from the center of the curvature. Then, from the geometry shown in Figure 7-15, we have:

$$2\tau sin(d\alpha/2) = \sigma_0 b dl = \sigma_0 b R d\alpha$$

Assuming : $\sin(d\alpha/2) = d\alpha/2$

$$R = \frac{\tau}{\sigma_0 b} \tag{7.35}$$

If the assumption stating that the line tension τ is independent of the orientation of the line holds, the previous relation means that the curvature radius of each element *dl* is a constant. As a consequence, the curvature of the arc AB is also constant, so that the arc AB is in the shape of an arc of a circle. Obviously, the arc AB at equilibrium cannot be obtained for any value of σ_0. Therefore, the curvature radius R must be longer than l/2 for a particular configuration to be stable. In other words:

$$R = \frac{\tau}{\sigma_0 b} \geq \frac{l}{2} \Rightarrow \sigma_0 \leq \frac{2\tau}{bl} \tag{7.36}$$

The arc AB can remain at equilibrium, in the "rest" position, as long as the shear stress σ_0 does not exceed the threshold stress $2\tau/bl$. If the stress σ_0 is greater than this limit, the equilibrium is broken, and the Peach-Koehler force prevails over the line tensions τ, leading to the dislocation bowing and forming the arc shown in Figure 7-16, creating a dislocation loop in addition to the segment AB.

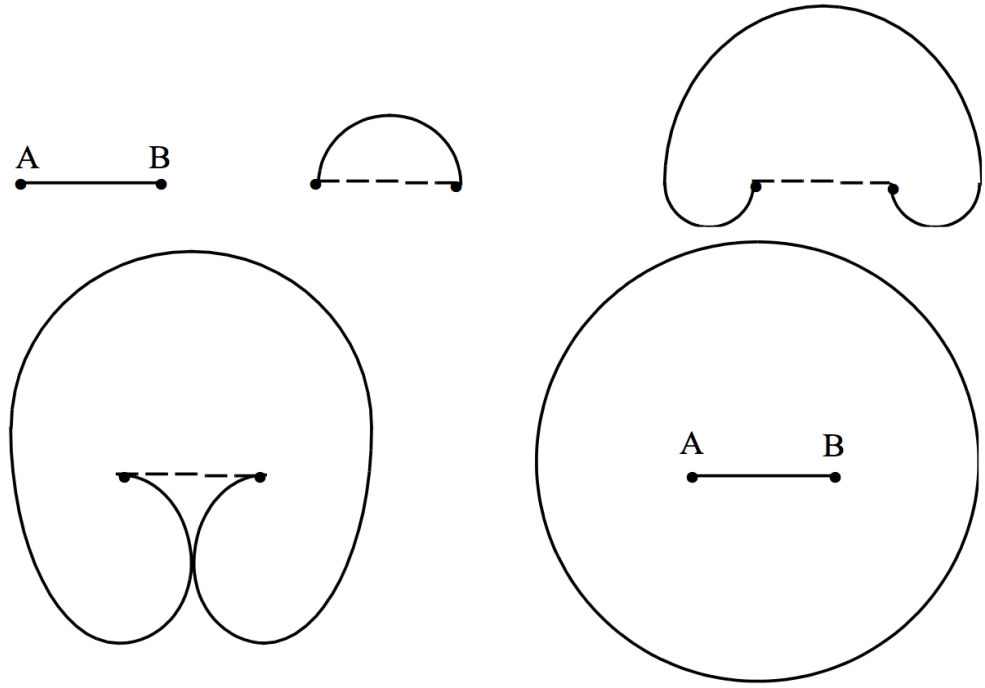

Figure 7-16: *Frank-Read source*

This process can continue if the stress on segment AB remains above the equilibrium critical value. This mechanism of dislocation multiplication is called the Frank-Read source. It is frequently observed in electron microscopy (Figure 7-16).

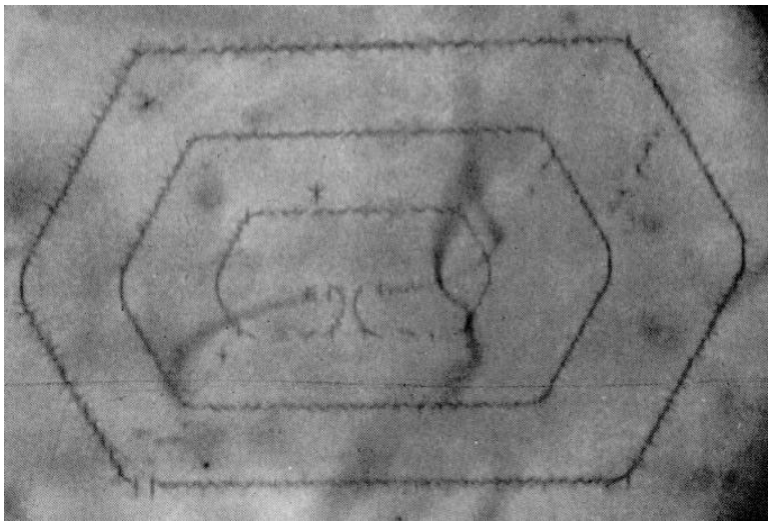

Figure 7-17: *Frank-Read source in Si decorated by Cu*

The stress required for dislocation multiplication via this mechanism is low. For a dislocation density $\rho \approx 10^{10}$ m/m^3, the average length of segment AB can be estimated as around 10^{-5} m.

Considering a line tension $\tau \approx 0.5\ \mu b^2$, we obtain a critical stress, $\sigma_0 = \frac{2\tau}{bl} \approx \frac{\mu b}{l} \sim 2.5 \cdot 10^{-5} \mu$ e.g., $\sigma_0 \sim 2.4$ MPa for copper.

7.6 Dislocations in FCC metals

The microstructure, i.e., the arrangement of dislocations in materials, depends heavily on the crystal structure. This section provides a more detailed description of dislocation arrangements within the FCC structure.

7.6.1 Shockley partial dislocations

FCC structures have sequences ABC ABC ABC {111} closed-packed plane stacking. The Burgers vectors of a perfect dislocation must join two lattice points. This vector must have a minimum length, so the most probable Burgers vectors are $a/2[110]$ to minimize the elastic energy of the dislocation.

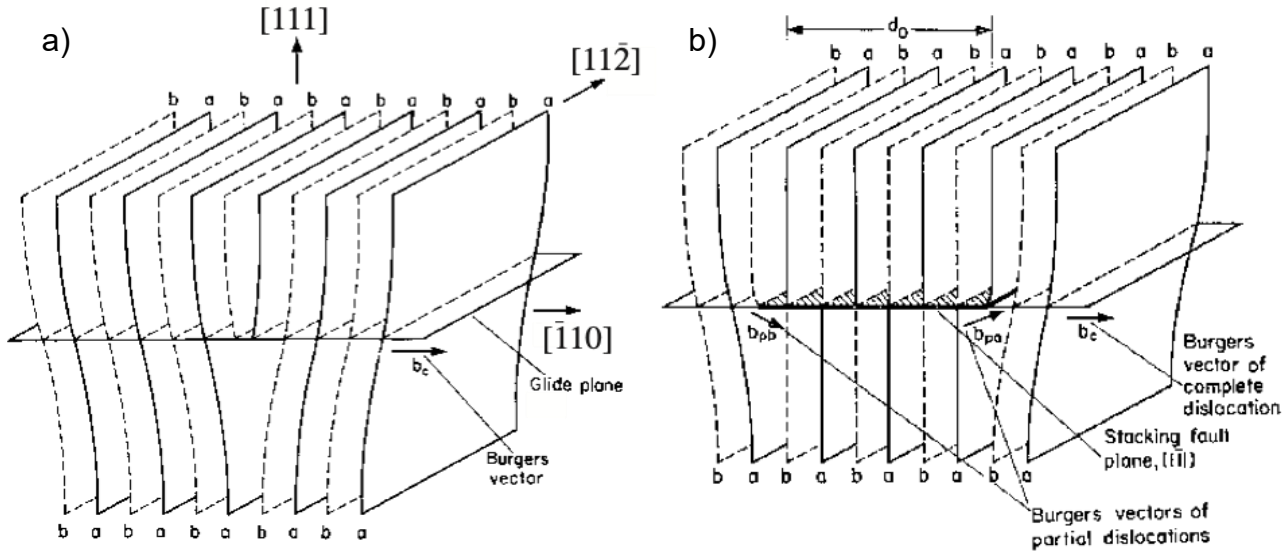

Figure 7-18: *A perfect dislocation is broken down into two additional planes (a) and in a dissociated dislocation (b)*

In Figure 7-18, we have represented an edge dislocation with Burgers vector $a/2[110]$, which comes from inserting two extra planes. The horizontal plane (dislocation plane) is the plane (111) on which we have represented the corresponding Burgers vectors. The dislocation has a direction $[11\bar{2}]$. We can understand that these two extra planes tend to repel and move apart, but we can also infer that this changes our physical understanding of dislocations.

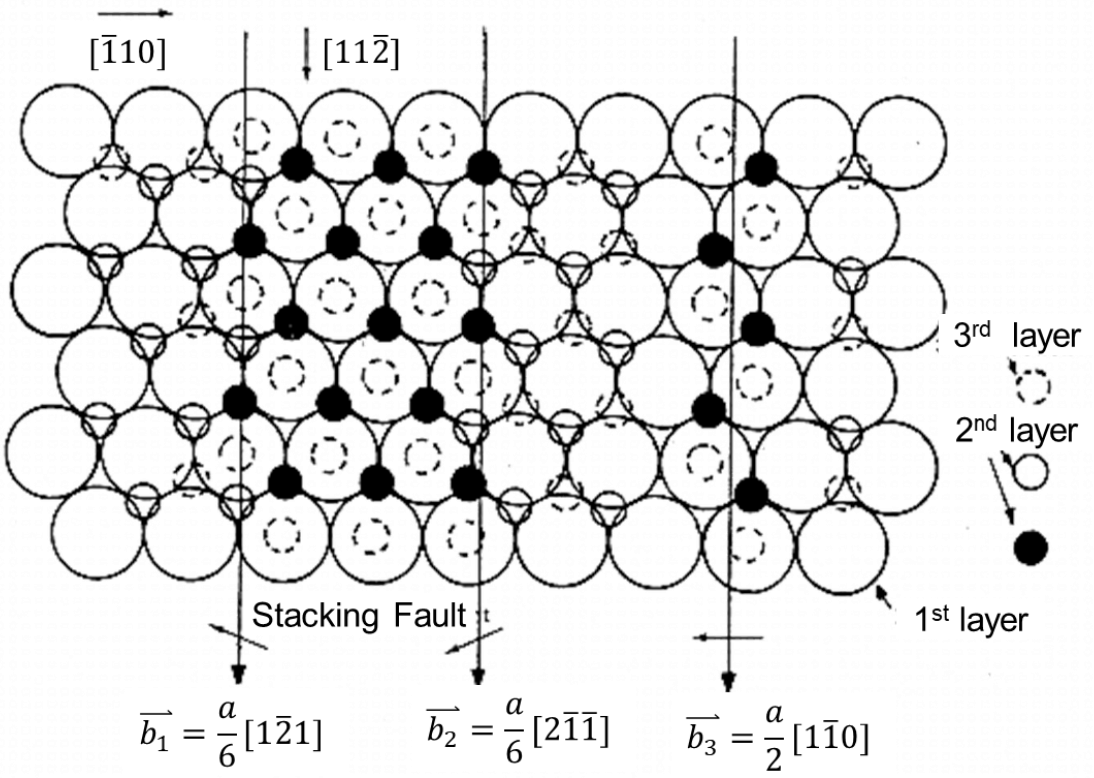

Figure 7-19: *Atomic arrangement in a stacking fault*

In Figure 7-19, we have tried to represent what happens when two planes move apart (Figure 7-19 is rotated by 90˚ compared to Figure 7-16). The big circles represent the first layer A (located just below" the dislocation). The small circles with solid lines represent layer B; they must be located initially on ∇ triangles, but two extra planes force the atoms between these planes to take place on Δ triangles (position C). The same applies to layer C, represented in Figure 7-19 by the dashed-lined circles. Thus, considering the stacking between the two inserted planes, we notice that it is found in the form:

We conclude that a stacking fault appears between the two inserted planes.
The dislocations that bound this defect are of a very particular kind: the Burgers vector associated with the one on the left is $\frac{a}{6}[2\bar{1}\bar{1}]$, and the one on the right-hand side has a vector $\frac{a}{6}[1\bar{2}1]$.
These are Shockley partial dislocations. We note that the initial perfect dislocation decomposes into two partial dislocations following Frank s formula:

$$\frac{a}{2}[1\bar{1}0] = \frac{a}{6}[2\bar{1}\bar{1}] + \frac{a}{6}[1\bar{2}1]$$

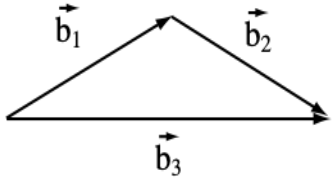

$$\vec{b} = \vec{b_1} + \vec{b_2}$$

We can see that this dissociation is energetically favorable because the angle between $\vec{b_1}$ and $\vec{b_2}$ is 120˚, and as a consequence:

$$b_1^2 + b_2^2 < b^2$$

We note that a partial dislocation has the following characteristics:

• Its Burgers vector is not a lattice vector,

• It is not surrounded by pristine crystal but bounds a stacking fault.

This second point forces us to revisit the energy problem raised earlier. If the two partial dislocations decrease their elastic interaction energy by moving away from one another, they create a stacking fault surface. Therefore, we can guess that the equilibrium position (the distance *d* between two dislocations) depends on the energy of the stacking fault γ (Figure 7-20).

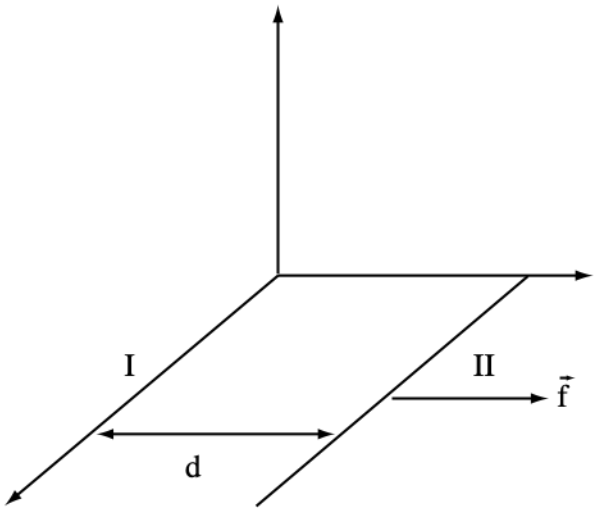

Figure 7-20: *Interaction between two dislocations determined by an equilibrium distance (the width of the defect)* d

At equilibrium, we have:

$$f\Delta x = \gamma\Delta x$$
$$f = \gamma \qquad (7.37)$$

We can show (exercise) that:

$$f_x = \frac{\mu}{2\pi d}\left[\frac{b_e^I b_e^{II}}{1-\nu} + b_s^I b_s^{II}\right] \qquad (7.38)$$

where the indices *e* and *s* indicate the edge and screw components of the Burgers vector of dislocations I and II. In the case of two Shockey dislocations:

$$b_e^I = b_e^{II} = \frac{a}{2\sqrt{2}} \qquad b_s^I = -b_s^{II} = \frac{a}{2\sqrt{6}} \tag{7.39}$$

Thus, (7.37) can be written as:

$$\frac{\mu b_e^2}{2\pi(1-\nu)d} = \gamma + \frac{\mu b_s^2}{2\pi d}$$

That gives:

$$d = \frac{(2+\nu)\mu a^2}{48\pi(1-\nu)\gamma} \tag{7.40}$$

Applications

Copper: $\mu = 4.85 \cdot 10^{11}\ dyne\ cm^{-2}$, $a = 3.62 \cdot 10^{-8}\ cm$, $d = 37\ Å$, $\gamma = 40\ erg\ cm^{-2}$, $\nu = 0.33$

Aluminum: $\mu = 2.8 \cdot 10^{11}\ dyne\ cm^{-2}$, $a = 4.05 \cdot 10^{-8}\ cm$, $d = 5.37\ Å$, $\gamma = 200\ erg\ cm^{-2}$, $\nu = 0.33$

Remark

Measuring the stacking fault width (d) by electron microscopy can be used to calculate the stacking fault energy (γ). However, measuring d < 10 Å using standard diffraction imaging techniques is challenging and requires aberration-corrected TEM, e.g., high-angle annular dark-field scanning TEM. This method cannot measure energies above γ = 5 erg cm-2 in these conditions. Therefore, this method does not apply to cases involving pure metals. On the contrary, in graphite, Delavignette and Amelinckx measured an energy of γ = 0.53 erg cm^{-2}.

7.6.2 Thompson tetrahedron. Frank partial dislocation, Lomer-Cottrell dislocation

a) Thompson tetrahedron

Using the Thompson tetrahedron, we can represent the groups of perfect and imperfect dislocations, along with their reactions, in an FCC structure. We use the fact that the four families of planes {111} can be represented by the four faces of a regular tetrahedron (Figure 7-21). Each edge corresponds to a vector, $a/2 < 110 >$, the Burgers vector of a perfect dislocation. The vertices of the tetrahedron are called ABCD. The face on the opposite side of A is called face *a,* and its center of gravity is α; the same goes for b and β, c and γ, d and δ for the faces on the opposite sides of the vertices B, C, D, respectively.

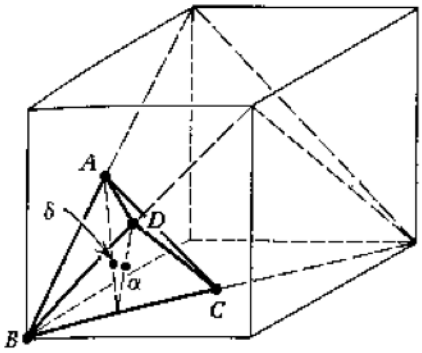

Figure 7-21: *Thomson tetrahedron*

This tetrahedron can be developed around the triangle ABC. The result is shown in Figure 7-22.

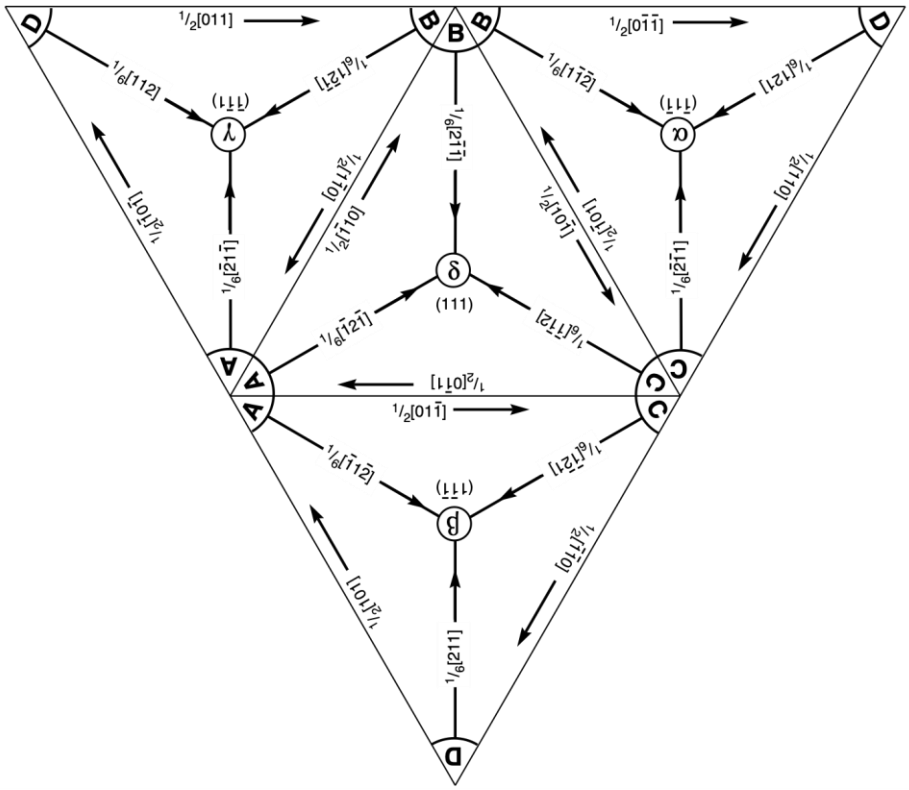

Figure 7-22: *Thompson tetrahedron expanded in 2D*

Two Latin characters represent the Burgers vector of perfect dislocations
($\overrightarrow{AB}=\frac{1}{2}[\bar{1}10]$ or $\overrightarrow{CD}=\frac{1}{2}[\bar{1}\bar{1}0]$); the Burgers vector of a Shockley dislocation can be represented by a Greek character and a Latin character, as follows: $\overrightarrow{\delta C}=\frac{1}{6}[11\bar{2}]$ $\overrightarrow{B\alpha}=\frac{1}{6}[1\bar{1}\bar{2}]$

Remark

The dissociation of a perfect dislocation into two Shockley partial dislocations associated with a Burgers vector $\overrightarrow{CB}$ and into a pair of vectors ($\overrightarrow{C\alpha},\overrightarrow{\alpha B}$); the very notion of pair implies that these

two terms are not interchangeable; in practice, this means that in Figure 7-19, we cannot interchange the Burgers vectors $\vec{b_1}$ and $\vec{b_2}$. In a more general way, we can give the following rule: When we look at the Thompson tetrahedron from the outside and dislocations in its positive direction, then this dislocation with Burgers vector $\overrightarrow{CB}$ dissociates into two partial Burgers vectors $\overrightarrow{C\alpha}$ to the right and $\overrightarrow{\alpha B}$ to the left. We invert these elements if we look at the Thompson tetrahedron from the inside".

Another way to remember this rule is to consider that a Latin-Greek $\overrightarrow{C\alpha}$" can be to the right, and a Greek-Latin $\overrightarrow{\alpha B}$" can be to the left.

b) Sessile Frank partial dislocation (Frank partial)

We have seen that an imperfect dislocation can be defined as the boundary of a stacking fault within the crystal. For a Shockley dislocation, if the stacking fault is created via sliding a close-packed plane on another, a stacking fault is made by taking away a part of a close-packed plane by condensing vacancies, for example. The boundary between the stacking fault and the perfect crystal is a Frank partial dislocation; its Burgers vector is average to the plane {111} of the stacking fault, and its modulus is in the form $a/3 < 111 >$. If we return to the Thompson tetrahedron, we note that $\vec{b} = \overrightarrow{A\alpha}$ for a stacking fault in the *A* plane.

Similarly, the precipitation of interstitials yields a Frank dislocation, which bounds an extrinsic stacking fault. We observe a substantial similarity between these Frank loops and the prismatic loops previously described. Nevertheless, a Frank dislocation cannot slide," as its glide plane is not of the {111} type. This dislocation is referred to as sessile." It can move, however, by a climb motion, even a conservative climb."

c) Lomer dislocation

Consider, for example, the planes a ($\bar{1}1\bar{1}$) and b ($1\bar{1}\bar{1}$). Their intersection is $\overrightarrow{CD}$ (Figure 7-23). Now, consider a perfect dislocation parallel to $\overrightarrow{CD}$ in each of these planes, their Burgers vectors are, respectively:

- $\overrightarrow{b_a} = \frac{a}{2}[10\bar{1}] = \overrightarrow{BC}$ for the dislocation in a
- $\overrightarrow{b_b} = \frac{a}{2}[0\bar{1}1] = \overrightarrow{CA}$ for the dislocation in b

For energy reasons, these two dislocations attract each other and form CD, a new perfect dislocation with the following Burgers vector:

$$\overrightarrow{BA} = \overrightarrow{BC} + \overrightarrow{CA} = \frac{a}{2}[1\bar{1}0]$$

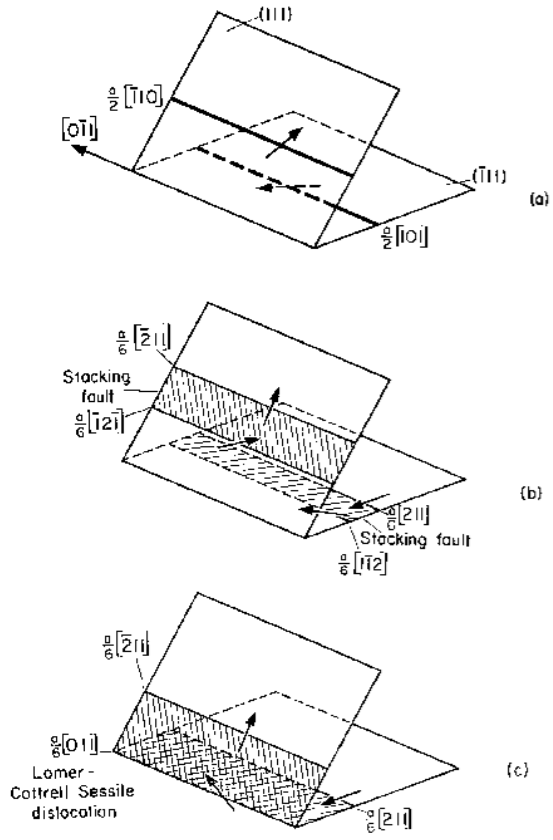

The two initial dislocations are of mixed type, whereas the resulting one is a pure edge dislocation.

The plane is defined by its direction, and the Burgers vector is the plane (1 0 0), which is not a glide plane in an FCC structure.

Consequently, this dislocation is sessile and is referred to as a Lomer dislocation. It is a barrier for other dislocations in planes (111) and ($\bar{1}11$). We also typically refer to this dislocation structure as a Lomer lock.

Figure 7-23 : *Formation of a Lomer lock (a) and recombination of Shockley partials forming a sessile Lomer dislocation*

d) Lomer-Cottrell dislocation

Consider now the same problem as before, but suppose that the stacking fault energy is low enough for the two initial perfect dislocations to dissociate into two Shockley imperfect dislocations in the following reactions:

$$\overrightarrow{BC} = \overrightarrow{B\alpha} + \overrightarrow{\alpha C} = \frac{a}{6}[1\,\bar{1}\,\bar{2}] + \frac{a}{6}[21\,\bar{1}]$$

$$\overrightarrow{CA} = \overrightarrow{C\beta} + \overrightarrow{\beta A} = \frac{a}{6}[\bar{1}\,\bar{2}1] + \frac{a}{6}[1\,\bar{1}2]$$

Considering the dissociation order (cf. previous remark), we arrive at Figure 7-23b. On CD, the two dissociated dislocations with Burgers vectors $\overrightarrow{\alpha C}$ and $\overrightarrow{C\beta}$ can combine (Figure 7-23c) and form a new dislocation with Burgers vector $\overrightarrow{\alpha\beta} = \frac{a}{6}[1\,\bar{1}0]$. This new dislocation is called a stair rod. The dislocation line is located along one side of the Thompson tetrahedron, and its Burgers vector is here in the form $\overrightarrow{\alpha\beta}$, joining the middle of the faces of this tetrahedron.

These dislocations (stair-rod) can also enable a different kind of reaction. For example, consider a dislocation line spanning from plane c to plane d and with Burgers vector $\overrightarrow{AB}$ (Figure 7-24).

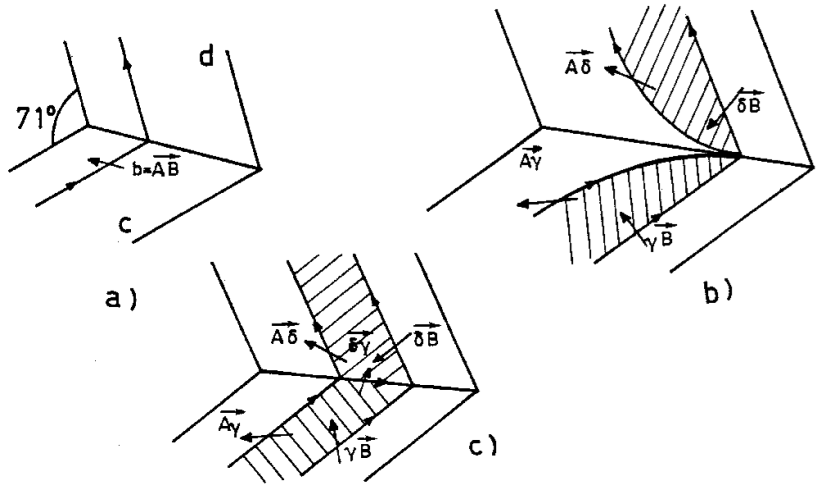

Figure 7-24: *Formation of a stair-rod dislocation at the intersection of planes with an acute angle*

This dislocation can dissociate in the c plane following the reaction $\overrightarrow{A\gamma}+\overrightarrow{\gamma B}$ and in the d plane as $\overrightarrow{A\delta}+\overrightarrow{\delta B}$. The dissociated dislocations at the intersection between two planes form a stair-rod dislocation with Burgers vector $\overrightarrow{\delta\gamma}$.

Not every stair-rod dislocation is in the form $\overrightarrow{\delta\gamma}$. For example, we choose an obtuse angle instead of an acute angle between the planes. Then, the dissociation of the dislocations is inverted on the plane seen from the outside of the Thompson tetrahedron (Figure 7-25).

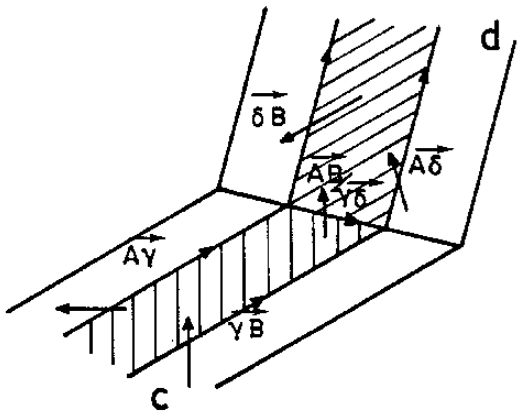

At the intersection between the two planes, the dissociated dislocations combine and form a stair-rod dislocation with Burgers vector $\overrightarrow{A\gamma}+\overrightarrow{B\delta}=\overrightarrow{AB}/\overrightarrow{\gamma\delta}$

We can also imagine stair-rod dislocations with a Burgers vector of the form:

$$\overrightarrow{\delta C}+\overrightarrow{D\gamma}=\overrightarrow{\delta D}/\overrightarrow{C\gamma}$$

or $\overrightarrow{\delta C}+\overrightarrow{\alpha D}=\overrightarrow{\delta\alpha}/\overrightarrow{CD}$

Figure 7-25: *Formation of a stair-rod dislocation*

Notation.

$\overrightarrow{PQ}$ represents the fixed vector linking P to Q. $\overrightarrow{PQ}/\overrightarrow{RS}$ represents a vector equal to twice the vector joining the middle of PQ to the middle of RS. We can show easily by vectorial operations that: $\overrightarrow{PR}/\overrightarrow{QS}=\overrightarrow{PQ}+\overrightarrow{RS}$

The conditions for the stability of these dislocations are related to the energy conditions (if $b^2 > b_1^2 + b_2^2$ dissociation occurs, if $b^2 < b_1^2 + b_2^2$ combination does). The displacement of stair-rod dislocations - in the glide plane as in the climb direction - is very difficult: these are super-sessile" dislocations, strong barriers against the motion of other dislocations.

7.6.3 Observation after quenching of samples at high and low stacking fault energy

In the micrograph shown in Figure 7-26, we observe a sample of aluminum quenched at 550˚C. The left image was taken immediately after the quenching and vacancy defects had gathered to form

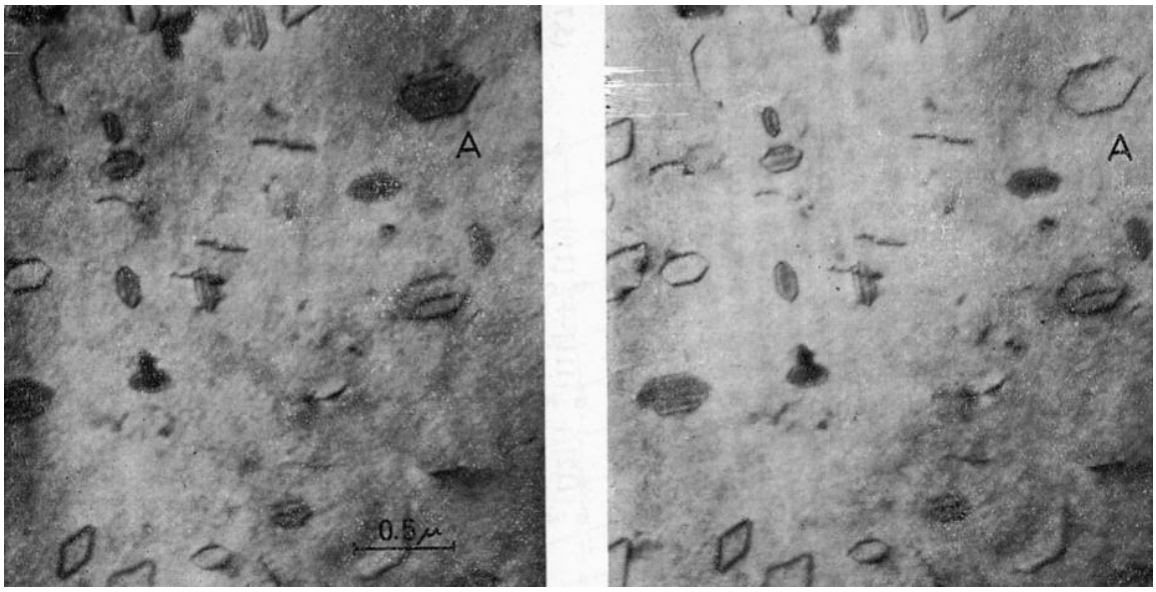

platelets surrounded by Frank dislocations.

Figure 7-26: *Sessile dislocation loops (Frank) in Al3.5%Mg. Micrograph a) is taken immediately after quenching from 550˚C to -20˚C. On the right (b), the sample has been heated in the microscope. We can observe the disappearance of the stacking fault A. The dislocation has become perfect*

The dynamical diffraction scattering contrast of stacking faults in TEM images appears as a set of characteristic stripes. The loops visible here are hexagonal, and the sides of the loops are parallel to the dense directions of the plane, $\langle 110 \rangle$. On the right, the sample has been annealed, and we observe that within one of the loops, the stacking fault has disappeared, but the profile remains; this can only be due to a perfect dislocation.

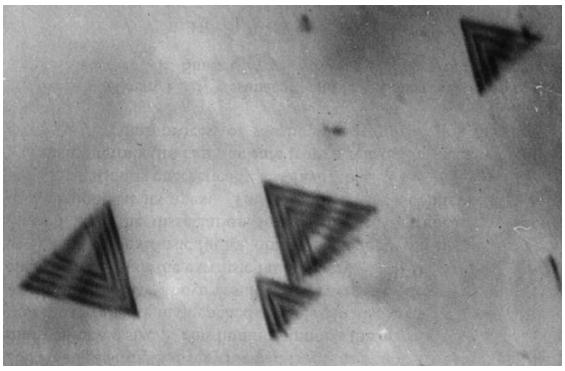

The micrograph in Figure 7-27 shows a gold sample that has also been rapidly quenched, though the result is quite different. Again, we observe defects in the shape of tetrahedra, characterized by sides that exhibit stacking faults.

Figure 7-27: *Tetrahedral loops in quenched gold.*

Such a difference between gold and aluminum should be attributed to differences in the energy of stacking faults in the two metals, which are very different ($\gamma_{Al} = 200$ erg/cm^2, $\gamma_{Au} = 10$ erg/cm^2). We now consider the two cases separately.

a) High stacking fault energy (Aluminum)

We assume the Frank dislocation loop is located in a {111} plane, and its Burgers vector is $\overrightarrow{\delta D} = \frac{a}{3}[111]$.

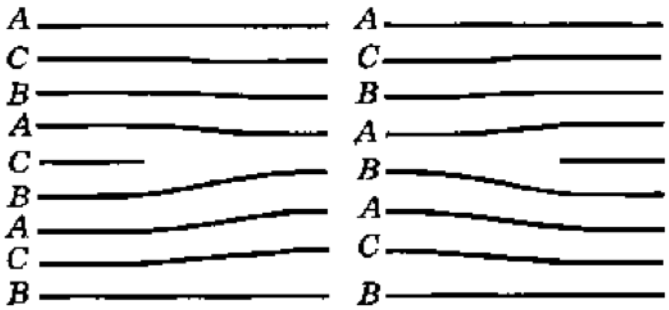

Figure 7-28: *Stacking fault in a Frank loop*

Considering Figure 7-28, we note that the stacking fault can be eliminated by moving the atoms from B to A and those from C to B, and so on.

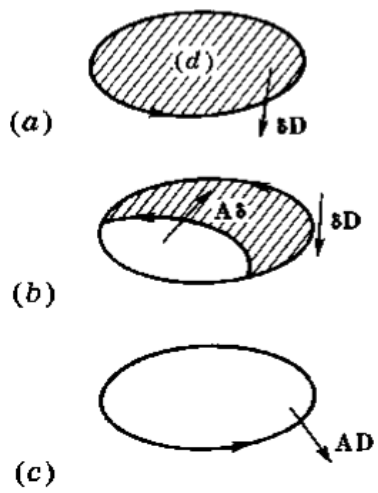

This operation is identical to creating a Shockley loop with Burgers vector and $\vec{b} = \overrightarrow{A\delta} = \frac{a}{6}[\bar{1}2\bar{1}]$ letting it grow within the defect (Figure 7-28).

The Shockley and Frank dislocations combine to give a perfect dislocation:

$$\overrightarrow{A\delta} + \overrightarrow{\delta D} = \overrightarrow{AD} = \frac{a}{2}[\bar{1}0\bar{1}]$$

This reaction is only possible if the stacking fault energy is high enough, which is the driving cause of the operation.

Figure 7-29: *Reaction between Frank and Shockley partial dislocations*

b) Low stacking fault energy (Gold) - tetrahedral defects

As for aluminum, an oversaturation of vacancies tends to reassemble into compact platelets following the planes {111} encompassed by a Frank dislocation. Although the stacking fault energy is low, a process similar to that in *Figure 7-29(a)* cannot occur. On the other hand, we can see that the sides of the defect orient along the close-packed directions, forming a triangular shape. If the base plane is a plane $(1\bar{1}1)$, a Frank dislocation has the shape drawn in Figure 7-30a with a Burgers vector.

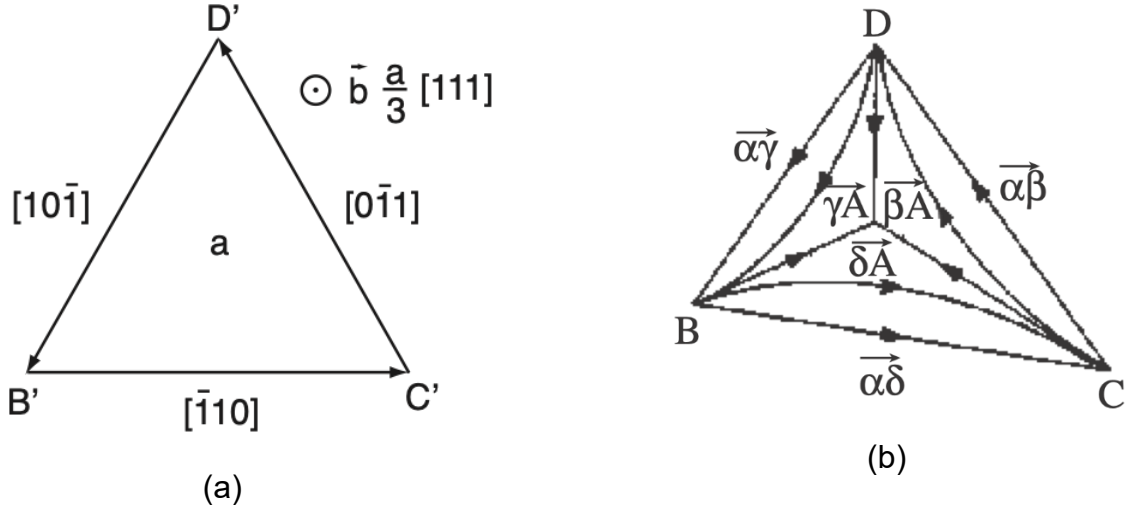

Figure 7-30: *Formation process of tetrahedral defects starting from a Frank loop*

Considering the dislocation B C , the Thompson tetrahedron indicates that this dislocation can dissociate in the *d* plane following the relation $\overrightarrow{\alpha A} = \overrightarrow{\alpha\delta} + \overrightarrow{\delta A}$, which is energetically favorable. In the same way, for C D and D B ',the Frank dislocation dissociates in a stair-rod dislocation and a Shockley dislocation (Figure 7-29b). The stair-rod dislocations are stable but push away the Shockley dislocations in their glide plane, creating a stacking fault between them (which does not matter much as the stacking fault energy is low). We can see in Figure 7-29b that Shockley dislocation B C and C D meet following A C Their combination is also energetically favorable, and the new Burgers vector is:

$$\overrightarrow{\beta A} + \overrightarrow{A\delta} = \overrightarrow{\beta\delta}$$

Similarly, following D'A' and B'A

$$\overrightarrow{\beta\delta} + \overrightarrow{\delta\gamma} + \overrightarrow{\gamma\beta} = 0$$

This final result is a tetrahedron completely bounded by intrinsic stacking faults and stair-rod dislocations of type $\overrightarrow{\alpha\beta}$.

7.6.4 Measure of the energy for a stacking fault

We have seen that, in theory, the stacking fault energy can be calculated from the dissociation distance of a dislocation (Figure 7.40). However, this method is only applicable for energies < 5 erg cm^{-2}. A slightly different method is possible because dislocations in a close-packed plane can interact and form junctions. In Figure 7-30a, we note that junction P is due to the intersection of three perfect dislocations with Burgers vectors $\overrightarrow{BC}, \overrightarrow{CD}, \overrightarrow{DB}$ in the plane ($\bar{1}1\bar{1}$). These three dislocations tend to dissociate and form an extended junction (Figure 7-31c). Figure 7-31 shows the formation of these extended junctions from the dissociation of partial dislocations.

The geometry of extended junctions is related to the stacking fault energy γ. As a first approximation, neglecting interaction forces between dislocations, we can state that the force due to the variation in

fault energy opposes the restoring force of the line tension from the Shockley dislocation at the junction boundary.

$$\gamma = \frac{\tau}{R}\,\gamma = \frac{\alpha\mu b_s^2}{R}$$

τ = line tension = $\alpha\mu b^2_s$, R = radius of curvature, b_s = Burgers vector of Shockley partial.

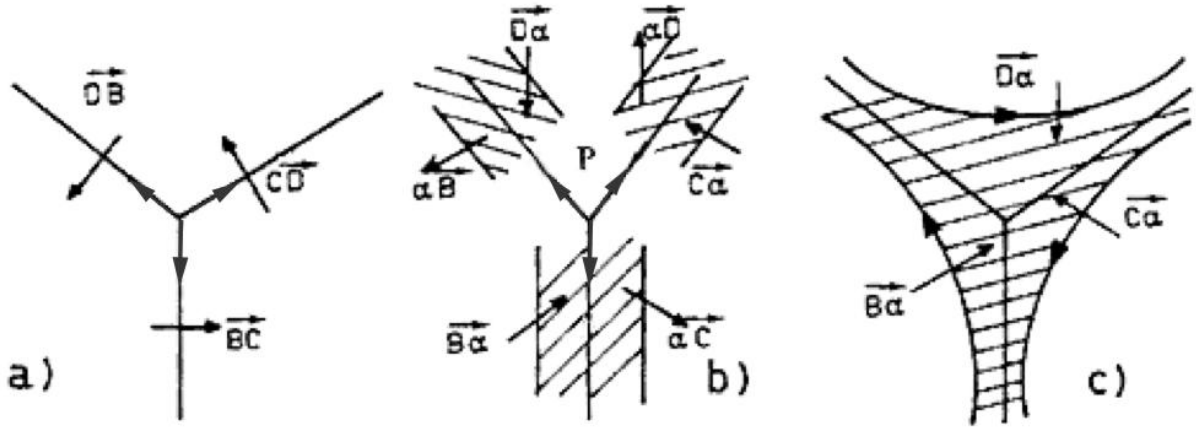

Figure 7-31: *Formation of an extended junction. The Thompson tetrahedron is seen from the outside.*

We can thus calculate γ by determining the curvature radius of the Shockley partial at the junction.

The junctions do not yield a representation similar to the one shown in Figure 7-31. If two dislocations with Burgers vectors $\overrightarrow{CD}$ and $\overrightarrow{DB}$ are permuted, we arrive at the case in Figure 7-32. We note that the partial dislocations (e.g., $\overrightarrow{D\alpha}, \overrightarrow{\alpha C}$) cannot recombine because they are in the wrong order. We do not obtain an extended junction; instead, a contracted junction is formed.

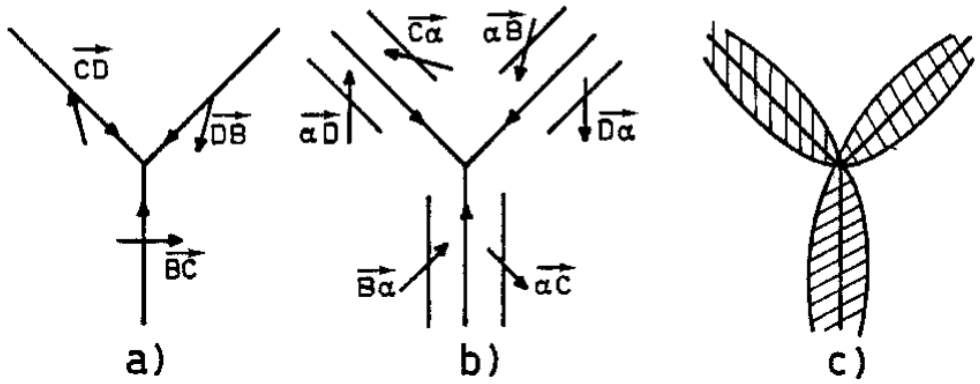

Figure 7-32: *Formation of a contracted junction. The Thompson tetrahedron is seen from the inside.*

Often, under the effect of the line tension, the dislocations located in a close-packed plane tend to rearrange into a hexagonal structure (Figure 7-33). In these conditions, we observe alternating extended and contracted junctions.

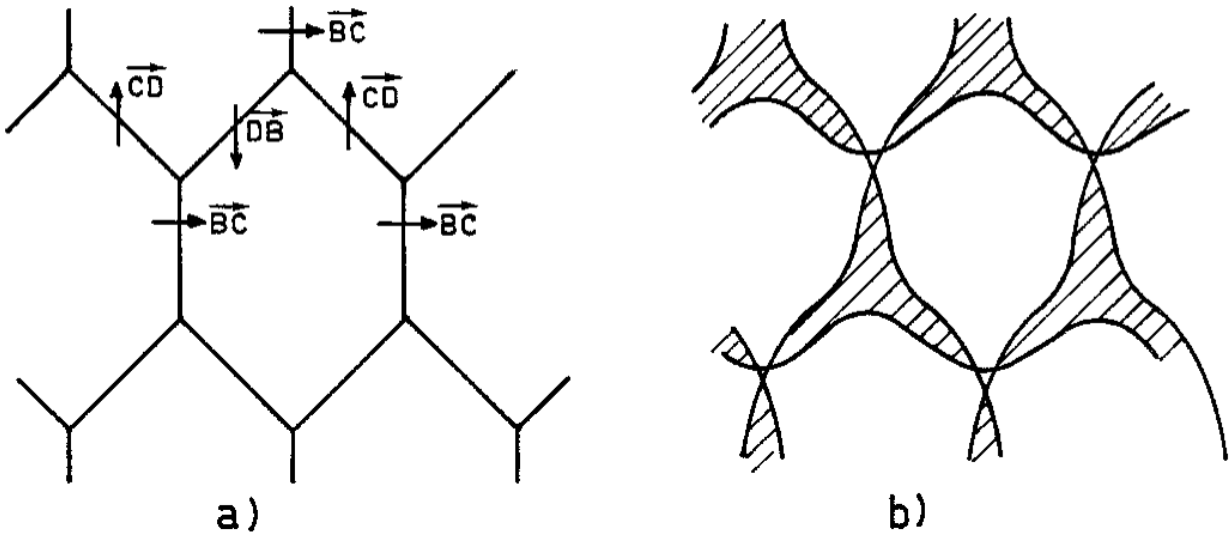

Figure 7-33: *Formation of a network of junctions*

Figure 7-34 shows an electron microscopy observation of hexagonal structured junction arrangements in a deformed Al-Cu alloy.

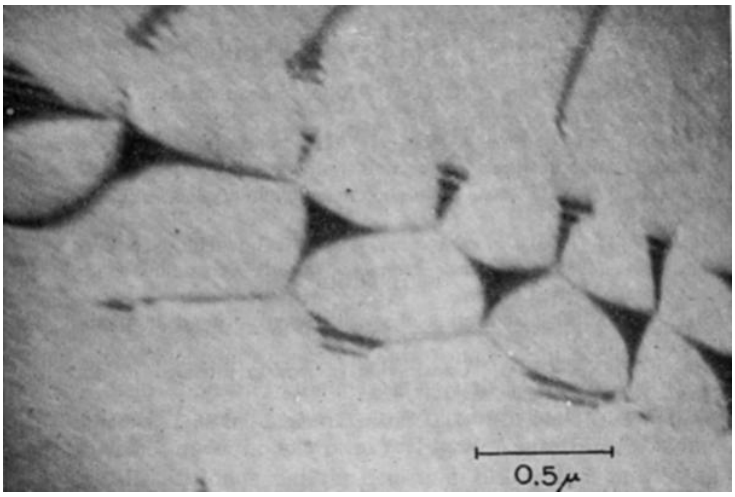

Figure 7-34: *Network of extended and contracted junctions observed in Cu8%Al after 5% strain*

7.6.5 Cross-slip

The dissociated dislocations tend to move as a whole, maintaining the width of the stacking fault constant. Therefore, it is hard to predict whether the Peierls stress is higher or lower in the case of dissociated dislocations or the presence of perfect dislocations. However, cross-slip is more complicated. In principle, dissociated screw dislocations cannot produce cross-slip because each imperfect dislocation has an edge component, and these must remain in their dissociation plane. On the other hand, partial dislocations may recombine, and they could change their glide plane by doing so.

In Figure 7-35, we have represented three stages corresponding to the cross-slip of a dissociated screw dislocation, which changes its glide plane from $(\bar{1}11)$ to $(1\bar{1}1)$. Initially, the dislocation contracts at a distance $2l_0$. Then, the dislocation now has a pure screw segment, and the cross-slip can develop in the plane $(1\bar{1}1)$. This phenomenon occurs especially when the dislocation encounters a barrier of sessile dislocations, causing the shrinkage of the stacking fault domain. Energy must be supplied to achieve this recombination; thus, cross-slip is more common in metals with high stacking-fault energy (e.g., Al).

This affects the behavior of metals during their deformation. In particular, since the formation of a constriction could be thermally activated, cross-slip increases with temperature.

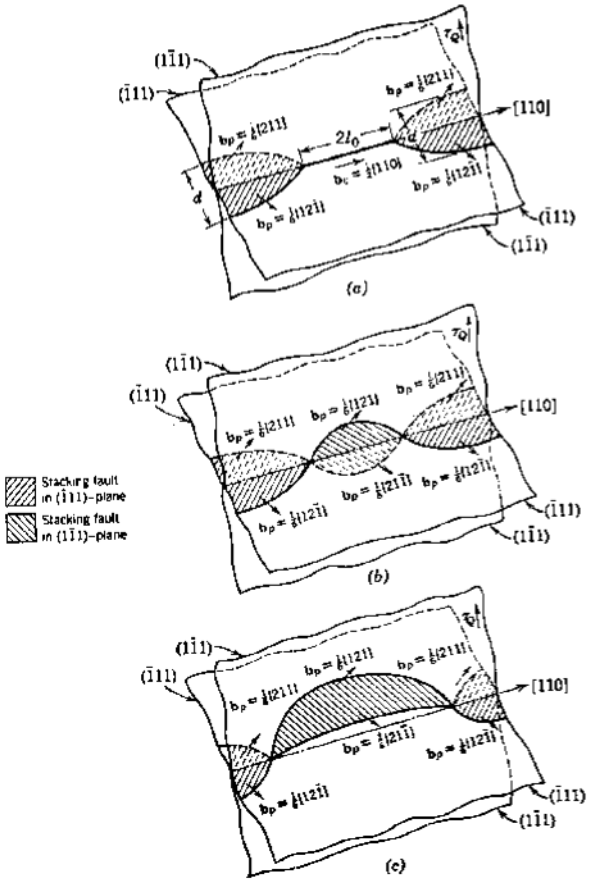

Figure 7-35: *Diagram of the cross-slip phenomenon in the presence of dissociated dislocations*

Regarding the intersection of two dissociated dislocations, we note that before crossing each other, they must recombine near their intersection, followed by a cut and creation of other jogs. Therefore, it is necessary to supply extra energy to create a jog in the presence of dissociated dislocations. This energy depends on the stacking fault energy. We can argue similarly for a stacking fault crossing a dislocation. Figure 7-36 shows some stacking faults in a copper alloy. The leading partial dislocations are blocked by the preexisting defects (arrow). Partial dislocations can also deviate, leaving behind stair-rod dislocations.

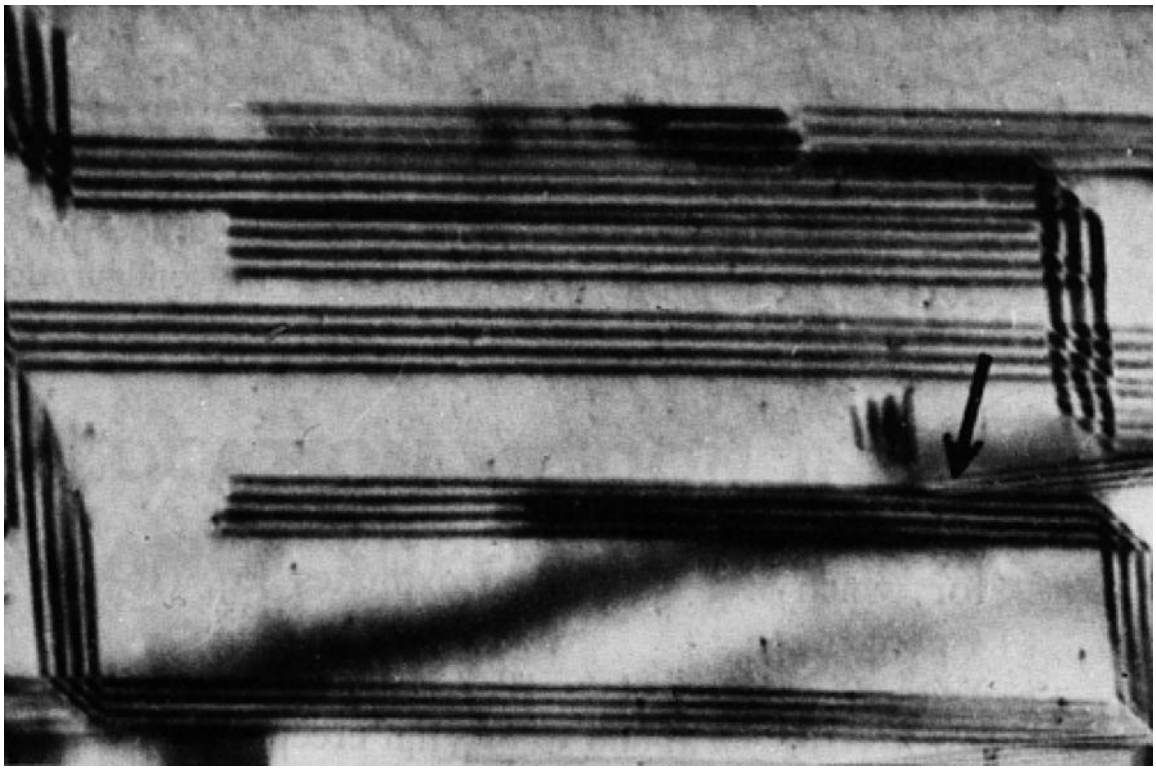

Figure 7-36: *Stacking faults and cross-slip in Cu-10%Fe*